Enhancing seismic resolution using continuous wavelet transform

Marcilio Castro de Matos*[1,2], and Kurt J. Marfurt[2]
[1]Sismo Research&Consulting; [2]The University of Oklahoma

This paper was prepared for presentation during the 12th International Congress of the Brazilian Geophysical Society held in Rio de Janeiro, Brazil, August 15-18, 2011.

Abstract

Most deconvolution algorithms try to transform the seismic wavelet into spikes by designing inverse filters that attempts to remove an estimated seismic wavelet from seismic data. Considering that seismic trace singularities are associated with acoustic impedance contrasts, and can be characterized by wavelet transform modulus maxima lines (WTMML), we show how to improve seismic resolution by using the wavelet transform. Specifically, we apply complex Morlet continuous wavelet transform (CWT) to each seismic trace and compute the WTMML's. Then, we reconstruct the seismic trace with the inverse continuous wavelet transform (ICWT) from the computed WTMML's with a slightly different complex Morlet wavelet than that used in the forward CWT. As the reconstruction process preserves amplitude and phase along different scales, or frequencies, the result resembles a deconvolution process. Using synthetic and real seismic data we show the effectiveness of the methodology on detecting seismic events associated with acoustic impedance changes.

Introduction

Deconvolution increases temporal resolution and yields a representation of subsurface reflectivity by compressing the basic seismic wavelet in the seismogram (Yilmaz, 2001). Most of existing deconvolution algorithms involve first estimating the seismic wavelet and then designing an inverse filter to remove these wavelets from the seismic trace (Lines and Ulrych, 1977). These algorithms also assume seismic traces can be modeled by convolving a basic seismic wavelet with the earth reflectivity (Yilmaz, 2001).

Deconvolution algorithm development is still an important research topic and, basically, consists on how to separate earth reflectivity from the seismic wavelet.

Nowadays, joint time-frequency, or spectral decomposition, filtering techniques are widely used to filter undesired noise such as ground roll and air waves (Matos and Osório, 2002). Filtering is implemented by exploiting the high redundancy of the joint time-frequency representation that, usually, maps the noise and signal to different regions of the time-frequency plane. The processor then identifies the noise component of the data, mutes it out or otherwise attenuates it, and reconstructs the signal from the remaining components.

Among several joint time-frequency techniques, the CWT is widely used and can be interpreted as a look up tool that enhances certain signal features at different scales, or frequencies. Using wavelet transform ridges detected along the scales, called the WTMML, Herman and Stark (2000), Matos et al. (2007), and Li and Liner (2008) showed how to characterize seismic trace singularities and how they can be associated with acoustic impedance contrasts.

Therefore, since the WTMML can be associated with earth reflectivity, we propose a CWT filtering algorithm that reinforces the acoustic impedance contrasts by shrinking the ICWT wavelet.

We begin our proposition by briefly reviewing WTMML theory and by showing how it can be associated with seismic singularities. Next, we present how the WTMML can be used to reconstruct a higher resolution seismic trace through ICWT. Then, we show how seismic interpretation can be improved by applying the proposed methodology to both synthetic and real seismic data.

The Methodology

The CWT was first formalized by Grossman and Morlet (1984) and is defined as the cross-correlation between the seismic trace and the dilated versions, at different scales, of a basic wavelet function with zero mean. The CWT can also be interpreted as the convolution between the seismic trace and the same (but time-reversed) basic scaled wavelets. In this manner we can interpret the CWT in the frequency domain to be a band-pass filter bank and, consequently, we can state that the CWT is a time-frequency, or, spectral decomposition technique.

After CWT computation, each seismic trace is transformed into a time (or depth) versus scale (or frequency band) matrix. Where, each matrix coefficient represents how well the seismic trace correlates to each dilated wavelet at each instant of time (or depth).

Later, Mallat and Zhong (1992) showed how the CWT can be used to detect multiscale edges by identifying modulus maxima lines (WTMML) along the scales and Tu and Hwang (2005) extended the same concept to complex wavelets. The manner in which the WTMML varies along the scales determines how sharp the edges are. Specifically, a parameter called the Lipschitz, or Holder exponent, is calculated by taken the inclination of the WTMML using logarithmic scale. Borrowing Mallat and Zhong hints, Herman and Stark (2000), and Li and Liner (2008) showed that the Lipschitz coefficients can be used

to characterize acoustic impedance contrasts when applied to seismic data with appropriate wavelet functions, while Matos et al (2007) used the whole WTMML to cluster different seismic facies.

Mallat and Zhong (1992) also showed that the original signal can be approximately reconstructed using a multiscale edge representation. In fact, the seismic trace can be reconstructed from its CWT coefficients by double integrating the coefficients times each dilated basic wavelet (Teolis, 1998). If a perfect trace reconstruction is not required then any wavelet function can be used with ICWT.

Assuming the WTMML is associated with important acoustic impedance contrasts, we propose in this paper to reconstruct each seismic trace directly from the detected WTMML's using a shrunken complex Morlet wavelet rather than the Morlet wavelet used in the forward CWT decomposition of the seismic data. In this manner, despite the different analysis and synthesis wavelet used, the CWT magnitude and phase are preserved and the ICWT reconstruction simply removes the wavelet side lobe effects of the main seismic events.

The proposed methodology is summarized below:

1- Compute the complex Morlet CWT of each seismic trace;

2- From the CWT magnitude, extract the WTMML that fall above an interpreter-defined threshold;

3- Compute the ICWT from WTMML coefficients using a shrunken Morlet wavelet.

Case 1: Synthetic seismic channel

To test this hypothesis we applied the proposed methodology to a 2D synthetic seismic response of a channel with thickness varying from 1ms to 50 ms convolved with a band-pass wavelet (Figure 1a).

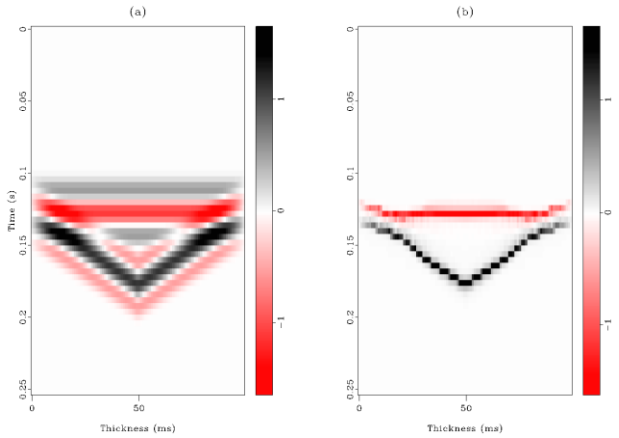

Figure 1: (a) Synthetic channel model and (b) its corresponding ICWT deconvolution.

Figures 2a and 3a show the synthetic traces at 10 ms and 30 ms thickness. Figures 2b and 3b show the corresponding ICWT-reconstructed traces. Figures 2c and 3c show the Morlet CWT magnitudes, which associated with Figures 2d and 3d, show that WTMML's detect the desired seismic events.

Applying this process to all the traces in Figure 1a we obtain the ICWT deconvolved image in Figure 1b. Note the improvement in temporal resolution of the proposed methodology.

By integrating the reflectivity series (Taner, 1992), we also calculated the relative acoustic impedance. Figure 4 shows the usefulness of relative acoustic impedance.

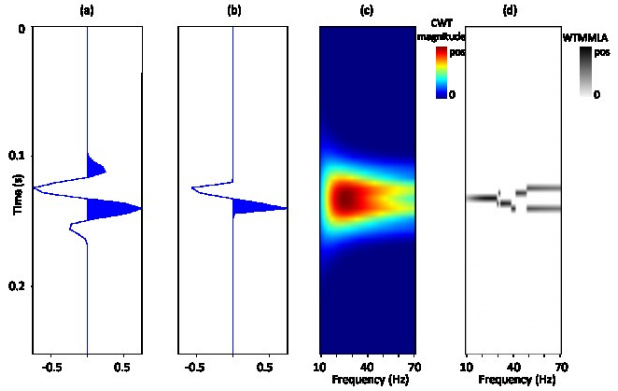

Figure 2: (a) 10 ms thickness trace; (b) ICWT deconvolution trace; (c) CWT Morlet magnitude; and (d) CWT modulus maxima.

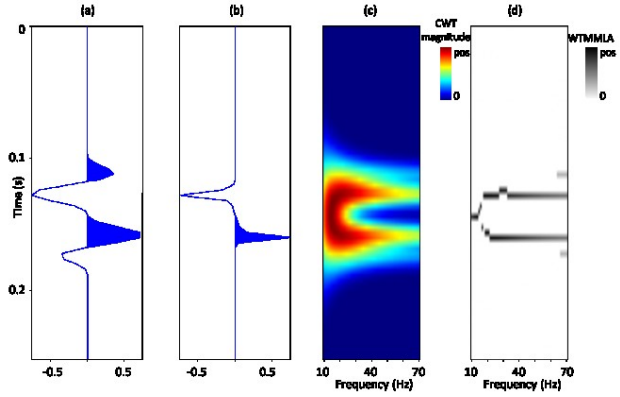

Figure 3: (a) 30 ms thickness trace; (b) ICWT deconvolution trace; (c) CWT Morlet magnitude; and (d) CWT modulus maxima.

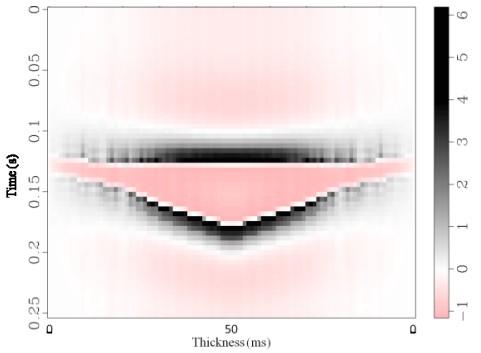

Figure 4: Relative acoustic impedance from ICWT deconvolution.

Figure 5 shows how the proposed algorithm also works well when we applied random additive noise to the same synthetic data.

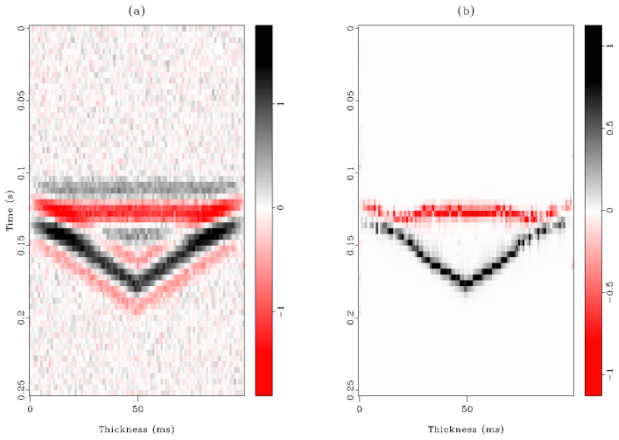

Figure 5: (a) Noisy Channel model and (b) corresponding ICWT deconvolution.

Case II: Synthetic from a random reflectivity series

The first example shows how the proposed algorithm can be applied to enhance seismic interpretation when applied to very simple three layer model. Next, we generate a pseudo random reflectivity series, 4ms sampled, and applied ICWT "deconvolution" to a 30 Hz Ricker wavelet filtered synthetic seismic. Comparing the reflectivity series in Figure 6a with Figure 6c, we can confirm the consistence of the result. As expected, components of the 30 Hz dominant frequency contaminate some of the reflectivity events. However, examining carefully the CWT magnitude (Figure 7a) and its corresponding WTMMLA (Figure 7b) we can identify most of the "stratigraphically" relevant events.

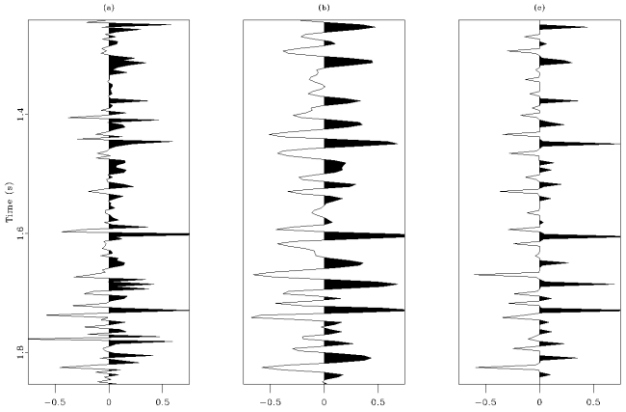

Figure 6: (a) Random reflectivity series; (b) Synthetic trace obtained by convolving (a) with a 30 Hz Ricker wavelet; (c) ICWT "deconvolved" trace.

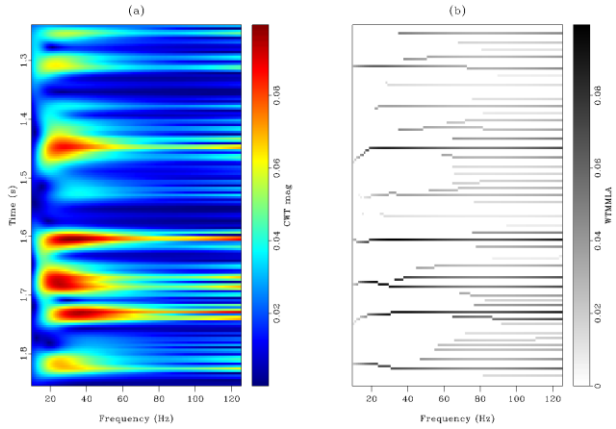

Figure 7: (a) CWT magnitude of the synthetic trace; (b) WTMMLA.

Case III: Marmousi2 synthetic data

Figure 8 shows Marmousi2 elastic model. This model was designed by Martin (2004) to evaluate AVO attributes after different seismic processing schemes. Different from our simple convolutional first example, Martin (2004) used elastic wave-equation forward modeling to keep realistic seismic events, like multiples, head waves, etc. In this paper, we used (Martin, 2004) the wave-equation prestack depth-migrated data set (Figure 9) to test our proposed algorithm.

Figure 10 shows the ICWT deconvolution result obtained using our algorithm from the seismic data illustrated in Figure 9, while Figure 11 shows relative acoustic impedance calculated from the deconvolved data.

Comparing Vp trace at CDP 500 as indicated in Figure 8 by a vertical dotted line (Figure 11a) with the respective seismic trace (Figure 11b) and the ICWT deconvolved trace (Figure 11c) we confirm the effectiveness of the proposed methodology. Figure 13a and 13b show the CWT magnitude and WTMMLA of the seismic trace.

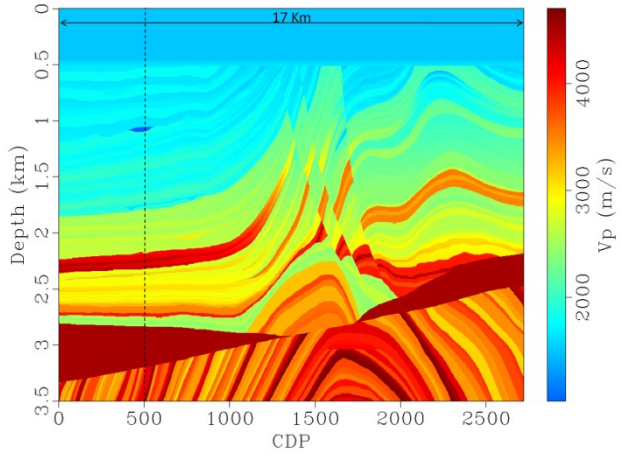

Figure 8: Marmousi2 Vp model (Martin, 2004).

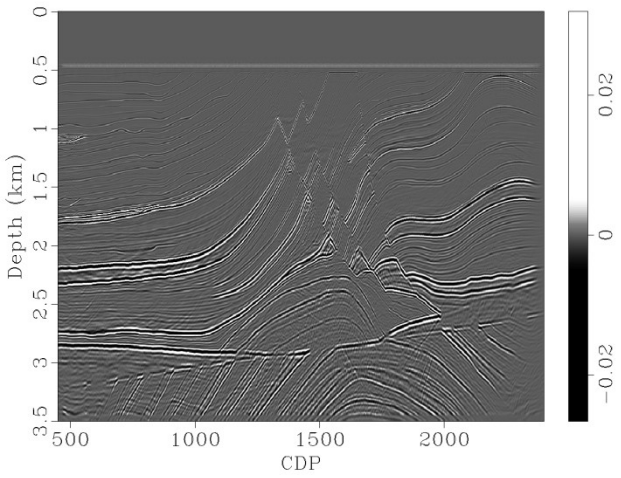

Figure 9: Wave equation pre-stack depth migrated synthetic seismic section from Marmousi2 model.

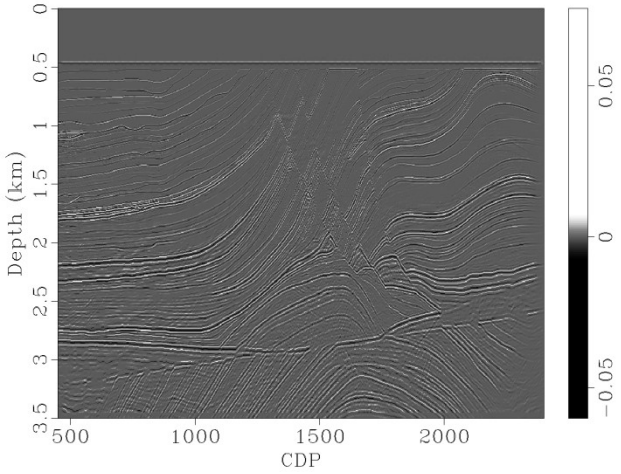

Figure 10: ICWT deconvolved section from Figure 9.

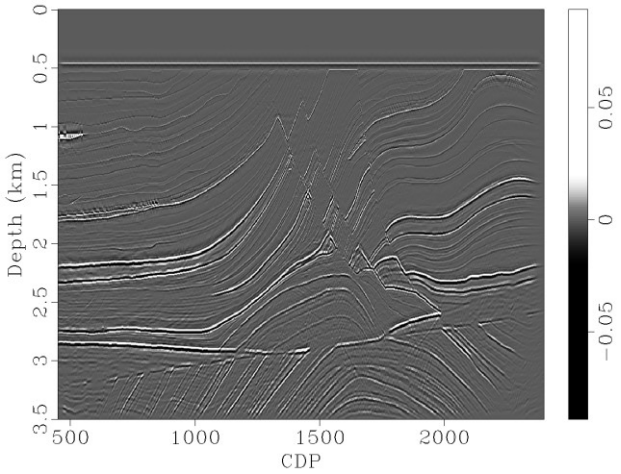

Figure 11: Relative acoustic impedance from Figure 10.

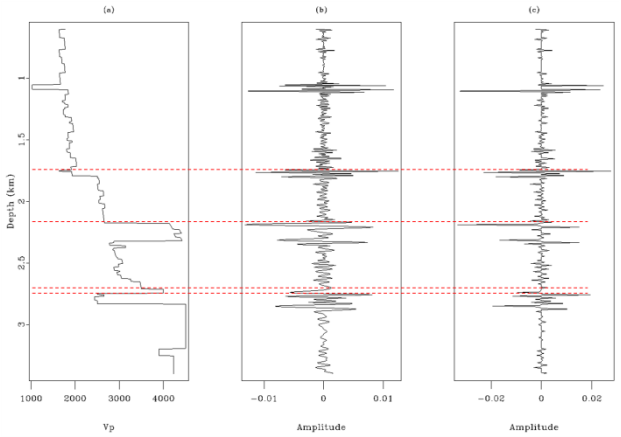

Figure 12: (a) Vp trace at CDP 500 from Figure 8; (b) Seismic trace at CDP 500 from Figure 9; (c) ICWT deconvolved data trace at CDP 500 from Figure 10.

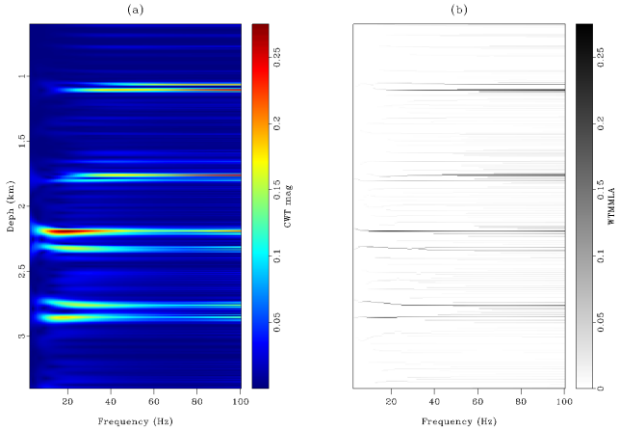

Figure 13: CWT magnitude (a) of the seismic trace illustrated in Figure 12d and its respective WTMMLA (b).

Case IV: Real seismic data

Finally, we applied the proposed methodology to the Boonsville dataset (Hardage, 1996). Comparing Figures 14a and 14b, it seems ICWT deconvolution result helps to discriminate better the limits of the main stratigraphic sequences. We can also notice that the seismic discontinuities, shown by vertical black arrows, along the reflector close to the time slice, indicated by a horizontal red arrow and by a white dot line, are better tracked by Figure 14b seismic line. These features represent karst caused by the dissolution of the underlying Ellenburger (Hardage, 1996).

As expected, ICWT "deconvolution" time slice illustrated in Figure 15b shows the contour of the karst features.

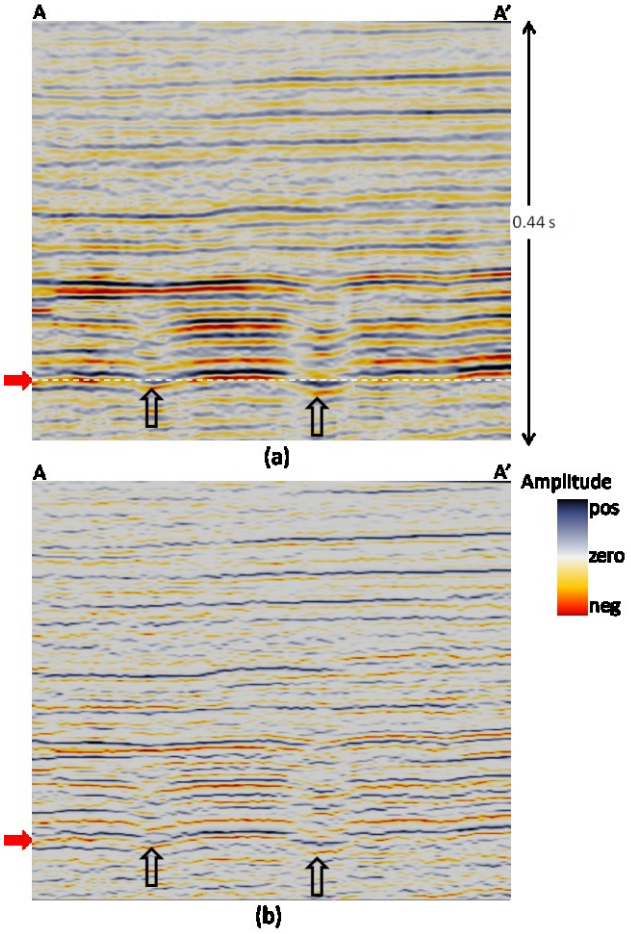

Figure 14: (a) Random seismic line AA' as indicated in Figure 15; (b) Random ICWT "deconvolution" line. Black vertical arrows indicate collapse features, while, red horizontal arrows indicate the level of the time slices shown in Figure 8.

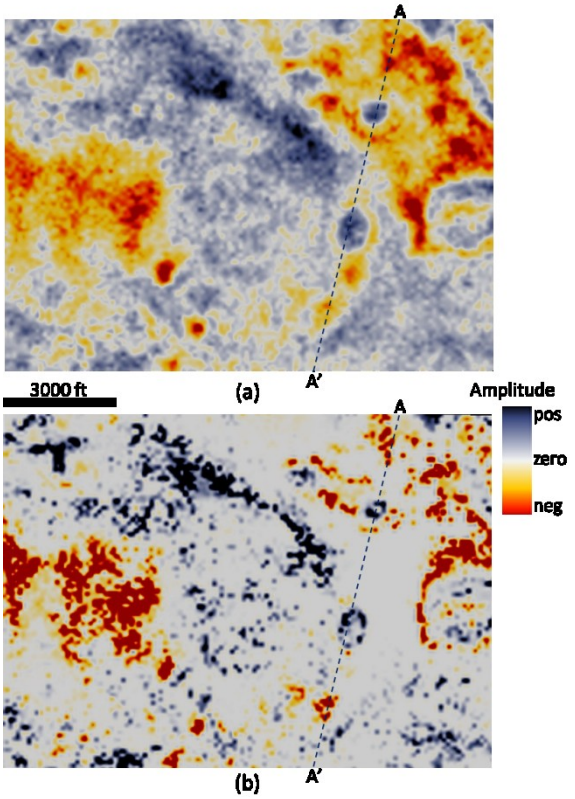

Figure 15: Time slices through the (a) amplitude and (b) corresponding ICWT "deconvolution" volume at t= 1.1 s indicated by the red horizontal arrow in Figure 7. Note the improved lateral resolution of the two karst features seen on the vertical line AA' displayed in Figure 7.

Conclusions

The CWT spectral decomposition filtering process described dear generates high resolution events that correlate to major acoustic impedance changes. Such higher resolution images can be particularly valuable in resolving difficult thin beds approaching the limits of seismic resolution. Since this broadening is a trace-by-trace independent process, laterally-consistent thin bed terminations and other truncations can be interpreted with confidence. As with all 'spectral broadening' algorithms, the results should be calibrated to well logs.

The spectrum of the forward complex Morlet wavelet should accurately express (and if desired, reconstruct) the bandwidth of the input traces. The CWT magnitude and the WTMML analysis of representative vertical slices should be examined to confirm if the chosen scales, (frequency band) and thresholds used to detect WTMML anomalies detect and delineate the features of interest.

In this paper, we reconstruct the seismic trace by preserving all the WTMML scales, giving rise to a broad-band reconstruction. We anticipate further analysis based on work by Goloshubin et al., (2006) to estimate measures of fluid mobility that are stronger at the lower frequencies.

Acknowledgments

The authors would like to thank industry sponsors of the University of Oklahoma Attribute-Assisted Seismic Processing and Interpretation (AASPI) Consortium.

References

Goloshubin, G., D. Silin, V. Vingalov, G. Takkand, and M. Latfullin, 2008, Reservoir permeability from seismic attribute analysis: The Leading Edge, **27**, 376-381, doi:10.1190/1.2896629.

Grossmann, A., and J. Morlet, 1984, Decomposition of Hardy functions into square integrable wavelets of constant shape: SIAM Journal on Mathematical Analysis, **15**, 723-736, doi:10.1137/0515056.

Hardage, B. A., 1996, Boonsville 3-D data set: The Leading Edge, **15**, 835-837, doi:10.1190/1.1437376.

Herrmann, F., and C. Stark, 2000, A scale attribute for texture in well and seismic data: 70th Annual International Meeting, SEG, Expanded Abstracts, 2063-2066, doi:10.1190/1.1815849.

Li, C., and C. Liner, 2008, Wavelet-based detection of singularities in acoustic impedances from surface seismic reflection data: Geophysics, **73** , V1-V9, doi: 10.1190/1.2795396.

Lines, L. R., and T. J. Ulrych, 1977, The old and the new in seismic deconvolution and wavelet estimation: Geophysical Prospecting, **25**, 512-540, doi:10.1111/j.1365-2478.1977.tb01185.x.

Mallat, S., and S. Zhong, 1992, Characterization of Signals from Multiscale Edges: IEEE Transactions on Pattern Analysis and Machine Intelligence, **14**, 710–732, doi:10.1109/34.142909.

Martin, G., 2004, The Marmousi2 model, elastic synthetic data, and an analysis of imaging and AVO in a structurally complex environment: M.S. thesis, University of Houston.

Matos, M. C., and P. L. M. Osorio, 2002, Wavelet transform filtering in the 1D and 2D for ground roll suppression: 72nd Annual International Meeting, SEG, Expanded Abstracts, 2245-2248, doi:10.1190/1.1817158.

Matos, M. C., P. L. M. Osorio, and P. R. S. Johann, 2007, Unsupervised seismic facies analysis using wavelet transform and self-organizing maps: Geophysics, **72**, P9-P21, doi:10.1190/1.2392789.

Taner, M.T., 1992, Attributes revisited, RockSolid Images, revisited 2000.

Teolis, A., 1998, Computational Signal Processing with Wavelets, 1st ed: Birkhäuser Boston.

Tu, C.L., and W.L. Hwang, 2005, Analysis of singularities from modulus maxima of complex wavelets: IEEE Transactions on Information Theory, **51**, 1049-1062, doi: 10.1109/TIT.2004.842706.

Yilmaz, Öz., 2001, Seismic Data Analysis: SEG.